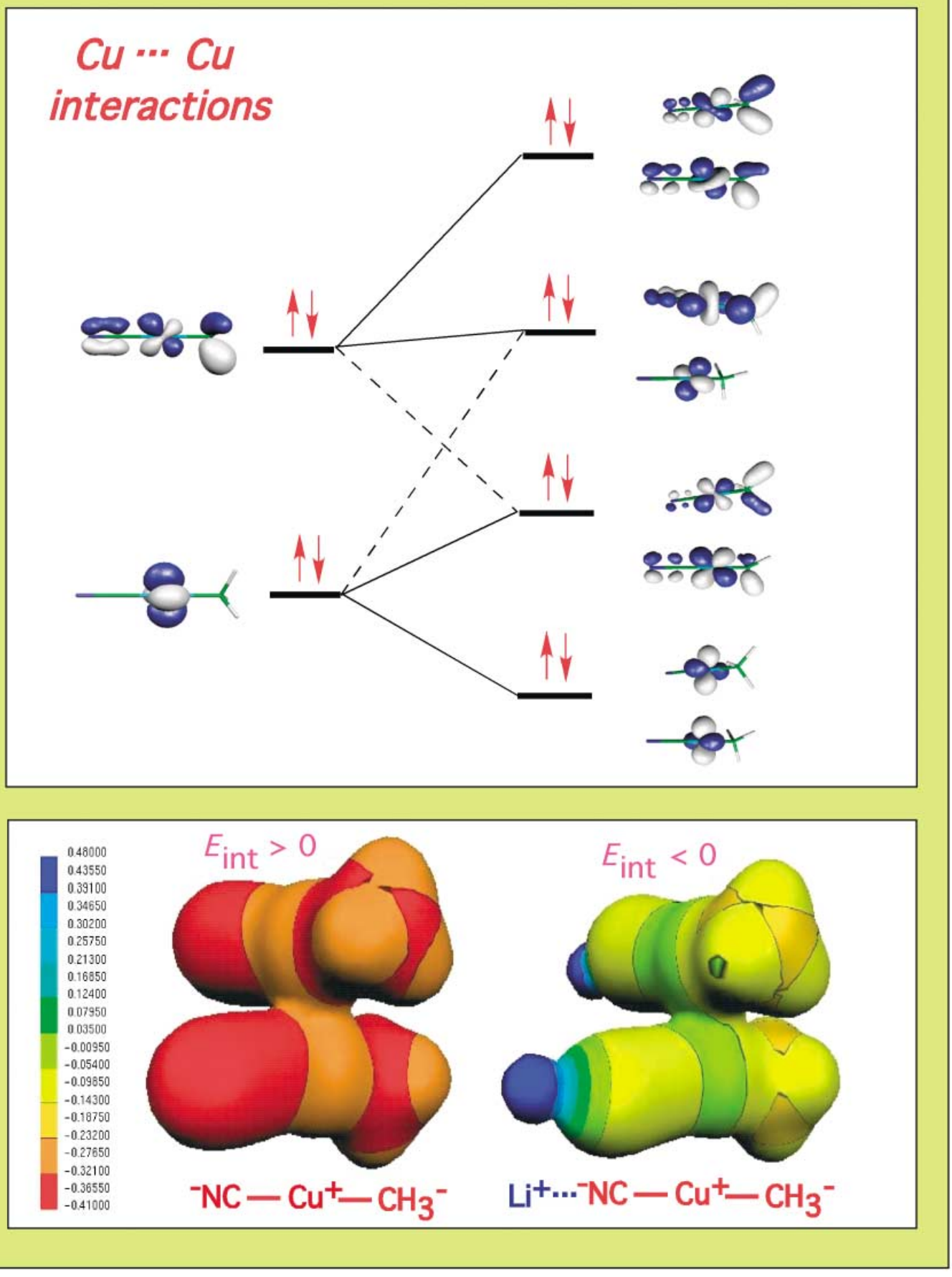

 DOI: 10.1002/chem.200305249

The Nature of Intermolecular $Cu^{I}\cdots Cu^{I}$ Interactions: A Combined Theoretical and Structural Database Analysis

M. Angels Carvajal,[a, c] Santiago Alvarez,[b, c] and Juan J. Novoa*[a, c]

Dedicated to Prof. José Vicente on the occasion of his 60th birthday

Abstract: The nature of intermolecular interactions between dicoordinate Cu^{I} ions is analyzed by means of combined theoretical and structural database studies. Energetically stable $Cu^{I}\cdots Cu^{I}$ interactions are only found when the two monomers involved in the interaction are neutral or carry opposite charges, thus allowing us to speak of bonding between the components of the bimolecular aggregate. A perturbative evaluation of the components of the intermolecular interaction energies, by means the IMPT scheme of Stone, indicates that both the Coulombic and dispersion forces are important in determining the $Cu^{I}\cdots Cu^{I}$ bonding interactions, because only a small part of that energy is attributable to Cu···Cu interactions, while a large component results from Cu···ligand interactions. The electrostatic component is the dominant one by far in the interaction between charged monomers, while in the interaction between neutral complexes, the electrostatic component is found to be of the same order of magnitude as the dispersion term. Bimolecular aggregates that have like charges are repulsive by themselves, and their presence in the solid state results from anion···cation interactions with ions external to this aggregate. In these cases, the short-contact Cu···Cu interactions here should be more properly called counterion-mediated Cu···Cu bonds.

Keywords: ab initio calculations · crystal engineering · metal–metal interactions · molecular recognition · noncovalent interactions

Introduction

The existence of metal···metal contacts shorter than the sum of the van der Waals radii between linear, d^{10} transition-metal complexes has been detected in recent years in a large number of crystal structures.[1,2] This is especially true for Au^{I} compounds, for which many contacts are found between 2.7 and 3.5 Å[3–5] (the sum of the van der Waals radii for Au is 3.40 Å), although the existence of these *short* contacts was recognized[6] as early as 1950 in Ag_2PbO_2 and $Ag_5Pb_2O_6$ (Ag···Ag distances of 3.07[6] and 2.97 Å,[7] respectively).[1] The overwhelming presence of such contacts in Au^{I} compounds lead Schmidbaur to coin the term *aurophilicity*.[8] By extension, it is common now to use *metallophilicity* to denote such contacts between metals in general, or *numismophilicity* to refer to the coinage metals.[9]

A look at the structures exhibiting $d^{10}\cdots d^{10}$ contacts shows that they exist in a wide variety of structural motifs. They can be found when the metal is two-coordinate (that is, in MXY complexes, X and Y being two monodentate ligands), in a variety of arrangements, for example, **1**–**12**.[10,11] Among them one can cite the supported and bridged intramolecular ones of types **1** and **2**. With respect to intermolecular (unbridged) $d^{10}\cdots d^{10}$ contacts, one can find cases where the ligands are connected through hydrogen bonds (**3**)[12,13] or ionic bonds (**4**),[14] mostly in eclipsed conformations, but also unsupported interactions either in a slipped arrangement (**5**) or in a staggered conformation (**6**). The number of contacts made by each metal atom goes from a single contact (**1**–**6**), to two contacts forming chains or rings (**7** and **8**), to larger

[a] M. A. Carvajal, Prof. J. J. Novoa
Departament de Química Física
Facultat de Química, Univ. Barcelona
Av. Diagonal 647, 08028-Barcelona (Spain)
Fax: (+34) 93-402-1231
E-mail: novoa@qf.ub.es

[b] Prof. S. Alvarez
Departament de Química Inorgànica
Facultat de Química, Univ. Barcelona
Av. Diagonal 647, 08028-Barcelona (Spain)

[c] M. A. Carvajal, Prof. S. Alvarez, Prof. J. J. Novoa
Centre Especial de Recerca en Química Teòrica
Parc Científic de Barcelona
Baldiri Reixach 10–12, 08028 Barcelona (Spain)
E-mail: novoa@qf.ub.es

Supporting information for this article is available on the WWW under http://www.chemeurj.org/ or from the author.

DOI: 10.1002/chem.200305249

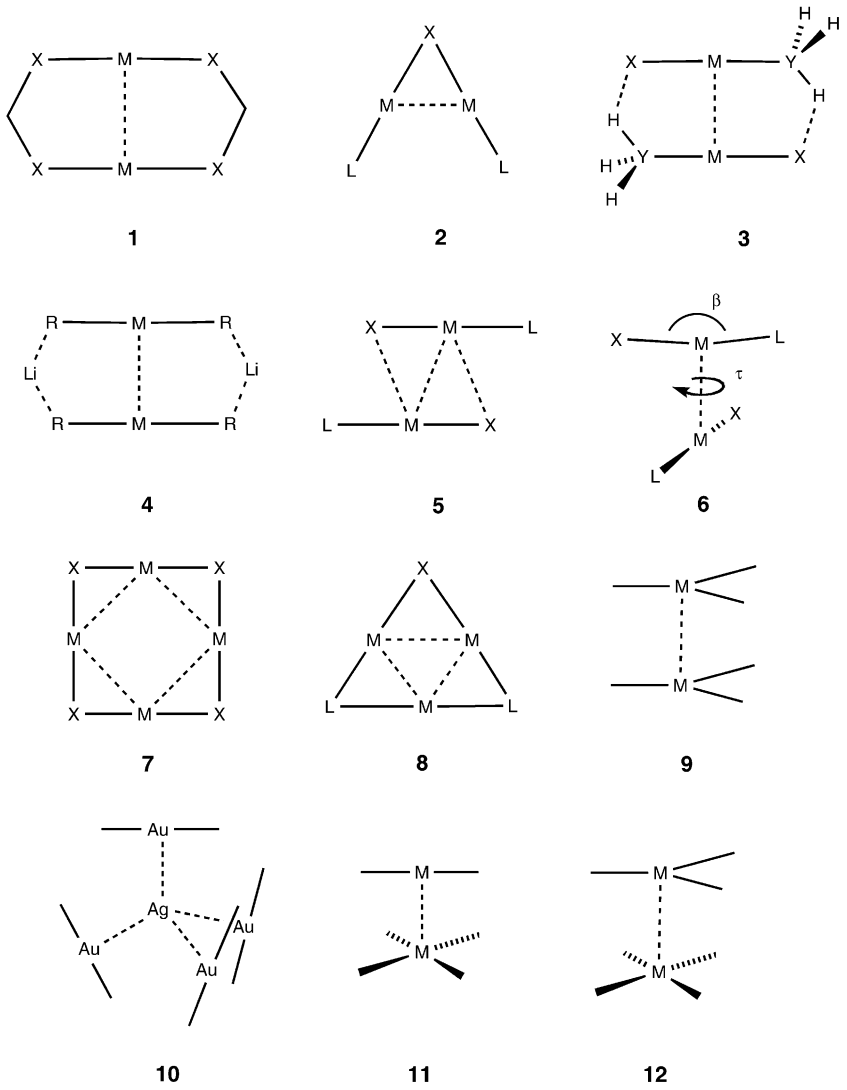

number of contacts (up to 6, extending in two or three dimensions).

The $d^{10}\cdots d^{10}$ contacts are not restricted to dicoordinate complexes nor to Group 11 metals. For instance, such contacts can be found in tricoordinate d^{10} compounds (**9**), which also show stacking interactions (e.g., Pt^0-,[15] Au^I-,[16] Ag^I-,[17,18] or Cu^I-bridged[19] complexes, or Ag^I in $RbAg_2As_3Se_6$[20]). Also Hg···Hg contacts in Hg^{II} compounds can be found at intra- or intermolecular distances as short as 2.84 Å[21] or 3.10 Å, respectively, to be compared with an atomic radii[22] sum of 3.54 Å. The most remarkable example of such contacts is probably to be found in the structure of $[\{Hg(SiMe_3)_2\}_2]$, a dimer with two linear molecules in a staggered conformation with Hg···Hg contacts of 3.146 Å.[23] A dimer of $[Pt(PPh_3)_2]$ has also been reported[24] and claimed to exhibit a Pt···Pt contact; however, its structure has not yet been resolved. Apart from these instances, we are not aware of contacts shorter than 3.8 Å between dicoordinate complexes of the Group 10 metals.

In addition to the homometallic contacts mentioned above, heterometallic contacts are also found (e.g., Cu···Hg = 2.689 Å[25] and Au···Hg = 3.085 Å[26]). A remarkable example of heterometallic contacts is that reported by M. Laguna and co-workers,[27] in which four linear Au^I complexes form contacts to a bare Ag^I ion in a tetrahedral fashion at 2.72–2.78 Å, reminiscent of the common coordination of four Lewis bases to such a metal ion (**10**). The closely related $d^{10}\cdots d^8$ interactions are also frequently detected. They were found as early as 1954 between linear and square-planar complexes (**11**),[28] and have already been reported for a variety of d^8/d^{10} pairs: Pd/Au, Pt/Au, Au/Au, Pt/Ag, Ir/Au, and Rh/Au.[29] Related $d^{10}\cdots d^8$ contacts are also found between trigonal-planar and square-planar complexes (**12**).[30]

Among the variety of characterized $d^{10}\cdots d^{10}$ contacts described above, we focus in this work on those between dicoordinate Cu^I ions. There are two main reasons for this choice: firstly, the amount of available data and theoretical studies is much more limited than that for the heavier elements in the same periodic group. Secondly, because of the fundamental interest in learning about the main differences between $d^{10}\cdots d^{10}$ interactions in the lighter metal in which relativistic effects are expected to be much less important. Compared to silver and gold (both have a similar atomic size), Cu is significantly smaller and, at the same time, relativistic effects are expected to be much less important. Therefore, we report here on a combined theoretical and structural database study of a variety of bimolecular aggregates with Cu···Cu contacts. While doing so, we will be searching for a general perspective rather than for quantitative data on specific examples. To that end, we present our study in three steps: 1) a detailed analysis of the crystal structures that present only one intermolecular Cu···Cu distance shorter than 3.7 Å, since these will constitute the best candidates for detecting unsupported Cu···Cu attractive interactions, 2) results of calculations at the MP2 level on bimolecular model compounds of the type schematically shown in **6**, 3) a perturbative analysis of the intermolecular interaction energy (with the IMPT formalism) of those model compounds, aimed at identifying the relative weights of the different contributions to the interaction energies.

Current status of the studies of $d^{10}\cdots d^{10}$ interactions: In addition to the above-mentioned structural data revealing short $d^{10}\cdots d^{10}$ contacts, a variety of other experimental and theoretical data related to this kind of interactions have been reported in the last few years. We present a brief summary in this section.

Spectroscopic evidence The 5d→6p transitions in the dinuclear complexes $[Au_2(dmpm)_2]$ and $[Au_2(dmpe)_2]$ (dmpm = bis(dimethylphosphino)methane, dmpe = bis(dimethylphosphino)ethane) appear at lower energies than in the analogous mononuclear complex $[Au(PEt_2)_2]^+$, a fact that has been attributed to the existence of Au···Au interactions in the former,[31] substantiated by magnetic circular dichroism spectroscopy. Ag_2SO_4, in which the Ag^I ions are hexacoordinate,[32] is colorless, whereas in solids with Ag···Ag contacts between dicoordinate Ag^I ions the absorption edges are shifted by up to 18000 cm^{-1} to lower wavenumbers, resulting in yellow and red compounds.[1] Consistently, all compounds with Ag^I aggregation are semiconductors, while Ag_2SO_4, with isolated Ag^I ions, is essentially an insulator. Moreover, for Cu^I delafossites, the activation energy for electrical conductivity is linearly correlated with the Cu···Cu distance.[1]

A band at $\tilde{\nu} = 88\ cm^{-1}$ in the Raman spectrum of $[Au_2(dcpm)_2]^{2+}$ has been assigned to Au–Au stretching[33] and the band at $\approx 100\ cm^{-1}$ in the spectrum of $[Ag(CN)_2]^-$ to Ag–Ag stretching.[34] The resonance Raman spectrum of $[Cu_2(dcpm)_2]^{2+}$ shows a peak at $\tilde{\nu} = 104\ cm^{-1}$ that has been assigned to Cu–Cu stretching.[19] We must also mention here that the energies of association between two monomers have been estimated to be in the range 7.5–12.5 kcal mol^{-1} from NMR[35–38] and visible[39] spectroscopy.

Theoretical studies: Let us try to describe the main aspects of the theoretical studies that deal with the nature of the $d^{10}\cdots d^{10}$ interactions between Cu, Ag, and Au.[2] Early semiempirical studies, based on extended Hückel calculations for dimers[40] and chains[41] of Cu^I and Au^I complexes, proposed a qualitative orbital model (**13**). In the absence of p–d hybridization, the d_{z^2} orbitals form σ and σ* combinations that are both occupied for the d^{10} complexes, and the empty p_z atomic orbitals give also σ and σ* combinations. This very simple model does not account for bonding between the two metal atoms, but is consistent with the red shift of the visible spectra and with the decreased energy gap for conductivity in dimers as compared to monomers. The assignment of the low-energy bands in the bridged dinuclear complexes $[Au_2(dmpm)_2]^{2+}$ and $[Au_2(dmpe)_2]^{2+}$ to a dσ*→pσ transition was confirmed by magnetic circular dichroism studies.[5] Mixing (hybridization) of the above two σ-type orbitals (**14**) results in stabilization of the occupied orbital as a consequence of its increased metal–metal bonding character. Similarly, mixing of the two σ* orbitals results in a stabilization of the occupied orbital as a consequence of its decreased antibonding character. The net result is that the repulsion between the d_{z^2} electrons becomes a weakly bonding interaction. A similar hybridization can be invoked for one of the metal–metal π-type orbitals.

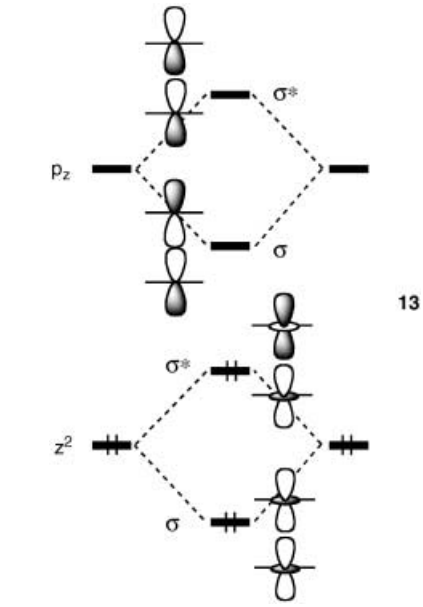

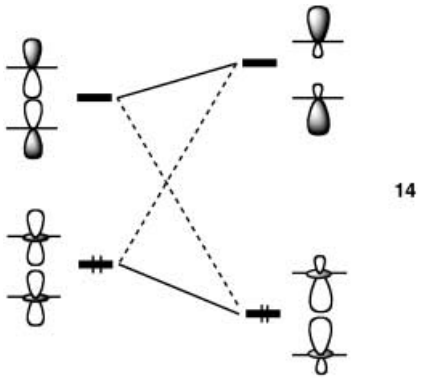

Ab initio calculations reported by Pyykkö and co-workers attributed the Au···Au interactions to correlation effects, because no attraction is found at the Hartree–Fock level; however, a weakly bonding interaction results when electron correlation is taken into account.[42,43] They also found that relativistic effects favor such interactions.[2] For a variety of perpendicular dimers (**6**) of $[AuX(PR_3)]$ complexes (X = F, Cl, Br, I, H, Me, CCH; R = H, Me)[44] they found interaction energies between −3.3 and −7.7 kcal mol^{-1}. The bonding energies in these series were seen to increase with the softness of the X ligand and, within the halides, also the Au···Au distance decreases with the softness of X. These results are the basis for the authors' claim that "the aurophilic attraction is a correlation effect". Further calculations[45] showed a dependence of the interaction energy on r^{-6} (where r is the metal···metal distance), consistent with a dispersive character of that interaction. A later analysis of the correlation at the local MP2 level[46] indicated that the largest portion of the correlation energy results from dispersion (that is, correlation associated to instantaneous polarization of the monomers), but also that a similar amount results from "ionic" contributions (i.e., those involving excited con-

figurations with ionic character, although the partitioning scheme used disregards ionic contributions corresponding to excitations of two electrons centered at the same metal atom). The fact that the correlation energy is not purely dispersion indicates that the Au···Au interaction is not purely van der Waals in nature. On the other hand, these calculations indicate that only about 40% of the correlation can be attributed to excitations within the d orbitals of the Au atoms, namely, there is an important Au···ligand contribution to the correlation energy. A recent study on $(H{-}M{-}PH_3)_2$ and $(Cl{-}M{-}PH_3)_2$ (M = Cu, Ag) dimers showed that similar conclusions can be reached for Cu···Cu and Ag···Ag interactions.[47] The influence of the ligands on the metal··· metal contact was previously analyzed at the extended Hückel level by Veiros and Calhorda.[48]

Ab initio studies of the $d^{10}\cdots d^{10}$ interaction in Cu^{I} complexes have been reported for the A-frame complex[49,50] $[Se(CuPH_3)_2]$ (**2**) and for the Cu_2X_2 diamonds (X = H, F, Cl)[51] (**15**). Little theoretical work, however, has been published for independent monomers besides the work of Magnko et al. mentioned in the previous paragraph. Within a study of a large number of gold compounds, Pyykkö et al. reported an interaction energy of $-3.1\,kcal\,mol^{-1}$ between two $[Cu(PH_3)Cl]$ molecules.[44] In a recent study of dimers of dicoordinate Cu^{I} complexes, we showed that the Cu···Cu attractive interaction is of the same order of magnitude compared to that of Au···Au interactions, and also, in many instances, these coexist with hydrogen bonding or compete with the formation of additional metal–ligand bonds.[52]

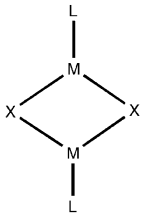

15

In a recent paper,[53] we theoretically analyzed the energetics and the influence of the geometry and ligands on the Cu···Cu interactions focusing on dimers of the $[\{CuX(NH_3)\}_2]$ type in a staggered conformation (X = Cl, Br, I, or CN). That study was carried out at the ab initio MP2 and B3LYP levels. The dissociation energies were found to be $\approx 2\,kcal\,mol^{-1}$, and the B3LYP calculations reproduced the MP2 results well, both at the qualitative and semiquantitative levels. However, in the presence of potentially bridging X ligands, the formation of rhombic structures (**15**) was found to be energetically favored, with calculated dissociation energies of 9–19 $kcal\,mol^{-1}$ for $[\{CuXL\}_2]$ dimers (L = NH_3, PH_3, or CNMe), even if the required bending of the linear monomers destabilizes the system by more than $20\,kcal\,mol^{-1}$. When the ligands allowed the formation of hydrogen bonds between the monomers, short intermolecular Cu···Cu interactions were possible, although these dimers were less stable than the rhombic structures **15**. The dissociation energies in the family of weakly associated dimers were found to increase with decreasing electronegativity of the halide ligand. It has also been shown that the interaction between two almost linear monomers becomes more stabilizing as the monomers are bent away from each other, although the net dissociation energy does not significantly vary on account of the destabilization resulting from bending the monomers away from their most stable linear geometry.[52,53]

Independently, Schwerdtfeger et al. reported MP2 calculations[54] on a variety of dimers of general formula $[\{CuL(CH_3)\}_2]$ (with L = OH_2, NH_3, SH_2, PH_3, N_2, CO, CS, CNH, and CNLi). These authors found interaction energies between monomers of up to $4\,kcal\,mol^{-1}$ and concluded that such intermolecular interactions are attractive, if approximately three times weaker than the analogous interactions between Au^{I} complexes. The effect of bending on the intermolecular interaction was also analyzed by those authors.[54]

It is also worth mentioning here that theoretical studies on similar weak interactions in extended solids, such as those found between linearly coordinated Cu^{I} ions of the two interpenetrated cristobalite-type lattices present in the cuprite structures of Cu_2O and Ag_2O.[55] Periodic ab initio calculations have been reported for Cu_2O, and the two independent cristobalite-like sublattices have been shown to be held through Cu···Cu contacts with a net attractive interaction of $\approx -6\,kcal\,mol^{-1}$ per formula unit ($-1\,kcal\,mol^{-1}$ per Cu···Cu contact). In the hexagonal $CuMO_2$ delafossites (M = Al, Ga, Y), the calculated and experimental electron-density maps indicate an accumulation of charge density in the center of triangles formed by three copper ions. Furthermore, the calculated map indicates the accumulation of density between each pair of copper atoms and a topological analysis of the electron density identifies these as ring and bond critical points consistent with the presence of bonding Cu···Cu interactions.[56] Comparison of these results with those discussed above on dimers clearly indicate that the same type of $d^{10}\cdots d^{10}$ bonding interaction exists in molecular and extended systems.

HF calculations on both the extended solids and in bimolecular models $[\{M(OH)(H_2O)\}_2]$, with a posteriori correction of the correlation energy by means of the LYP functional, and MP2 calculations on the latter, consistently predict bonding energies of $\approx$1–5 $kcal\,mol^{-1}$ per M···M contact. A Bader analysis of the electron density of a bridged Ag^{I} complex identified the existence of bond-critical points connecting the two Ag ions,[57] thus indicating the existence of a bonding interaction between these two atoms in that compound, consistent with the presence of $d^{10}\cdots d^{10}$ interactions.

Luminescence: Further experimental evidence for the bonding nature of $d^{10}\cdots d^{10}$ interactions came from luminescence studies.[58,59] The first report of luminescence of M^{I}–phosphane complexes (M = Cu, Ag, Au) was published in 1970.[60] Although it has been shown that luminescence itself is not necessarily associated with the existence of Au···Au interactions,[61] it has been noted that mononuclear Au^{I} complexes generally show luminescence only in the solid state,[62] thus suggesting that the formation of intermolecular

contacts is needed to produce luminescence. A recent study by Fackler has shown a strong dependence of the emission spectrum on the gold–gold interaction for S–Au–S dinuclear complexes.[63] The concentration dependence of the red shift of the absorption edge of $[Au(CN)_2]^-$ in solution[64] is consistent with the orbital perturbation brought about by the Au···Au contacts. A similar interpretation can be given to the different luminescence[65,66] of the Cs^+ and K^+ salts of $[Au(CN)_2]^-$: while the former presents two contacts per Au atom at 3.11 Å and luminescences at $\lambda = 458$ nm, the latter has four contacts per metal at a much longer distance (3.64 Å) and the luminescence appears at $\lambda = 390$ nm. For more reports on the decreased energy of the luminescence of dicyanoaurate in the solid state, see the references cited by Rawashdeh-Omary et al.[64]

Large Stokes shifts (of the order of 6000 cm^{-1})[61] in the luminescence spectra of compounds with Au···Au contacts are consistent with the σ* and σ nature of the HOMO and LUMO in the dimers (**13**). Luminescence in thiolato Au^I complexes, [LAu(SR)], is thought to originate from ligand-to-metal charge-transfer (LMCT) excited states;[67] however, even in those cases, the pσ empty orbital is thought to be responsible for the luminescence (**16**). A recent experiment by

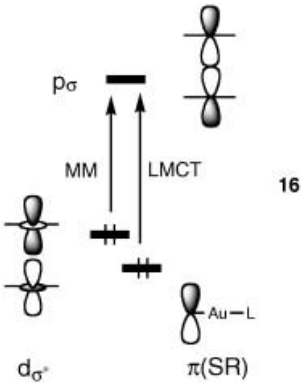

16

Yam et al.[68] demonstrated this on a benzocrown-functionalized thiolato–Au^I dinuclear complex **17**: a Au···Au contact is formed upon addition of K^+ with a concomitant shift of the luminescence band from $\lambda = 502$ to 720 nm, consistent with the stabilization of the pσ orbital in **13** as a result of the intermetallic interaction.

Stokes shifts of 9000 cm^{-1} are typical of Cu^I complexes, although the excitation giving rise to luminescence is sometimes assigned to a ligand-to-metal charge transfer or to a $3d^{10} \rightarrow 3d^9 4s$ transition.[69] A relationship between the presence of Cu···Cu contacts and a luminescent behavior, similar to that found for Au compounds, has also been proposed.[70]

Structural evidence of Cu···Cu interactions in the solid state

On account of the scant attention devoted so far to the structural aspects of Cu···Cu interactions and prior to discussing the possibility of the existence of Cu···Cu bonding interactions, we analyze the available structural data that should be included in our theoretical study and which serves as a guide for the selection of model systems to compute. To this end, we carried out a search in the Cambridge Structural Database (CSD)[71] of compounds that exhibit only one intermolecular Cu···Cu contact between 2.0 and 5.0 Å, thus disregarding those exhibiting more than one Cu···Cu contact, as well as those with bridging ligands between the two Cu atoms, because, in the presence of bridging ligands, a short Cu···Cu distance may be geometrically imposed and not the result of an attractive interaction (e.g., **1**, **2**, **7**, and **8**). For comparison, we carried out a separate search for intramolecular contacts. The distribution of the Cu···Cu distances in both types of contacts is presented in Figure 1. An

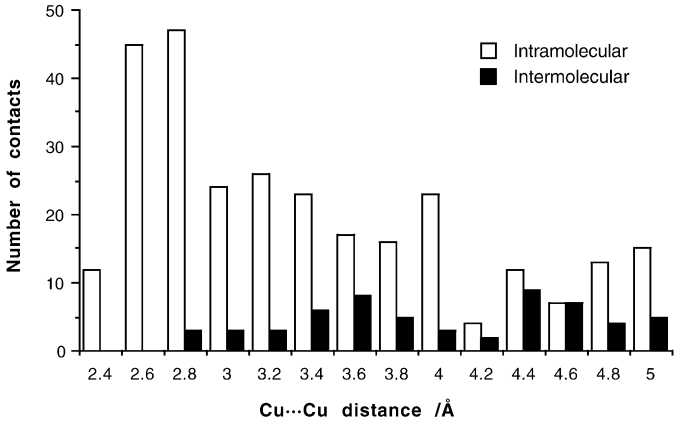

Figure 1. Distribution of Cu···Cu distances among dicoordinate complexes as found in the Cambridge Structural Database (version 5.23). Intermolecular (black bars) and intramolecular (white bars) contacts are represented separately.

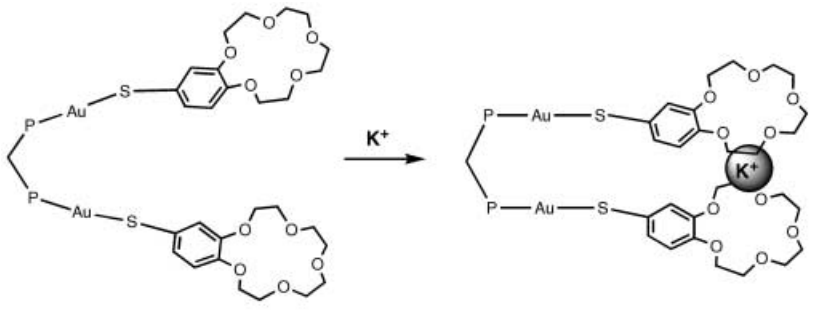

17

additional search was also carried out for Cu^I complexes defined in the CSD as being tricoordinate with a Cu–Cu bond.

The distribution of intramolecular contacts (Figure 1) shows that the bridged dinuclear compounds exhibit distances as short as 2.38 Å with a maximum at ≈2.8 Å, to be compared with a van der Waals radii sum of 2.80 Å.[72] These bridged compounds correspond

to a variety of topologies from dinuclear to polynuclear compounds, including some common motifs, such as the cyclic structures obtained with small polyatomic bridging ligands (**1**), A frames (**2**), triangles (**8**), or squares (**7**) obtained with monoatomic bridges, or more complex structures with higher nuclearity, up to a Cu_{32} aggregate.[73] A similar assortment of intramolecular contacts can be found in purely inorganic solids. Thus, we can find the A frames (**1**) in the isolated $[Cu_2S_3]^{4-}$ anions of $Na_4Cu_2S_3$ and in the zigzag chains of $BaCu_2O_2$, or in molecular oxo-bridged squares in LiCuO.

Intermolecular contacts show a distribution similar to that found for the intramolecular ones, but now the shortest distance is 2.71 Å (compared to 2.38 Å for intramolecular contacts), which is slightly below the sum of the van der Waals radii. This suggests that intermolecular Cu···Cu contacts can be attributed to the presence of attractive interactions between the Cu atoms. The distribution of intermolecular contacts presents a maximum at ≈3.6 Å and drops to a minimum at 4.2 Å. Thus, in what follows, we will focus our attention on the shortest distances (Table 1) with a cutoff of 3.7 Å.

Table 1. Experimental structural data (distances [Å], angles [°]) for compounds with one intermolecular Cu···Cu contact shorter than 3.7 Å.

Compound[a]	Cu···Cu	X	L[b]	τ	Cu···X	β	Ref.
$[CuL_2]^+[CuX_2]^-$ (cation···anion)							
rukhua	2.810	Cl	pyfc	85.5	3.579	176.9	[96]
sawxap	3.611	Cl	Me_3py	89.0		180.0	[97]
$[\{CuXL\}_2]$ (neutral···neutral)							
vijmuw	2.944	Me_2pz		61.1	3.368	173.5	[98]
	2.977			61.4	3.388	173.6	
cadziq10	3.014	Cl	η^1-tp	176.5	2.618	159.2	[99]
vusvua	3.070	Me_3pz	Me_3pz	60.3	3.495	173.8	[100]
kalkaj	3.362	Br	tmpip	180.0	3.762	173.7	[101]
	3.635			174.1	3.754	174.2	
newqah	3.584	CR_3	CR_3	5.4	3.685	167.2	[74]
$[\{CuL_2\}_2]^{2+}$ (cation···cation)							
	3.002		bpp	7.5	3.680	167.4	[102]
taghak	3.199		nmIm	4.0	3.685	173.6	[103]
pewyof	3.292		RIm	45.7	3.688	173.3	[104]
	3.425			42.3	3.739	169.3	
lefpan	3.466		Me_2Im	0.0	3.658	179.1	[105]
capgef	3.483		pzMe	180.0	3.603	178.1	[106]
$[\{CuX_2\}_2]^{2-}$ (anion···anion)							
nutbej	2.713	Bu, CN		85.6	3.203	169.0	[75]
	2.922	Cl		82.5	3.249	165, 171	[107]
rixmeq	3.223	$RCOO^-$		3.5	2.756	171.6	[108]
newqah	3.584	CR_3		5.4	3.685	167.2	[74]

[a] CCDC code. [b] bpp = 1,3-bis(4-pyridyl)propane; RIm = substituted imidazole; nmIm = *N*-methylimidazole; pyfc = 1,1′-bis(2-pyridyl)octamethylferrocene; pzH = pyrazole; pz^- = pyrazolato; tmpip = 2,2,6,6-tetramethylpiperidine; tp = tris(pyrazolyl)borate.

In the above description of our database analysis of the $d^{10}\cdots d^{10}$ contacts, we paid no attention to the net charge of the molecules hosting the copper atoms. As we will show below, the net charge of the fragment is the decisive factor in defining the energetics of the intermolecular interaction associated with the shortening of Cu···Cu contacts. Consequently, there is no reason to expect that the geometrical features of the Cu···Cu contacts should be the same in neutral and charged compounds. Therefore, we have classified the intermolecular Cu···Cu contacts shorter than 3.7 Å in Table 1 according to the net charge of the interacting monomers. From here on, we will refer to anionic ligands as X and to neutral ligands as L, whereupon the net charge of the monomers is unambiguously identified from their general formulae, namely, neutral [CuXL], anionic $[CuX_2]^-$, or cationic $[CuL_2]^+$. However, in some cases, the assignment of a net charge to a monomer is not straightforward, particularly in compounds in which a Li^+ ion is attached to an anionic ligand.[74,75] Therefore, we can choose to consider the combination of ligand and cation as a neutral ligand or, instead, consider only the anionic ligand as forming part of the complex—the option adopted here. The present classification shows that "short" contacts (<3.0 Å) present in the cation···anion and neutral···neutral families, are not found among the cation···cation dimers (the shortest contacts in these families are placed at 2.810, 2.944, and 3.002 Å, respectively), whereas the shortest contact corresponds, rather surprisingly, to an anion···anion dimer (2.713 Å) found in one of the Li^+ salts.

To gain a wider perspective on the existence of short $d^{10}\cdots d^{10}$ contacts, we have also searched for contacts in the crystal structures of dicoordinate complexes of the following d^{10} ions: Ni^0, Pd^0, Pt^0, Ag^I, Au^I, Zn^{II}, Cd^{II}, and Hg^{II}. The search was restricted to metal–metal intermolecular contacts at less than 4.0 Å, and only one contact per metal atom. No such contacts were found for Ni^0, Pd^0, Pt^0, Zn^{II}, and Cd^{II}. For Ag^I, Au^I, and Hg^{II}, the shortest contacts were found at 2.96, 2.94, and 3.10 Å, respectively.

The nature of the interactions between Cu^I monomers The systematic analysis of the crystal structures that exhibit short Cu···Cu contacts presented in the previous section has allowed us to identify the existence of four types of bimolecular aggregates with intermolecular Cu···Cu contacts: neutral $[\{CuXL\}_2]$ dimers, charged $[\{CuL_2\}_2]^{2+}$ and $[\{CuX_2\}_2]^{2-}$ dimers, and $[CuL_2]^+[CuX_2]^-$ ion pairs. In this section, we will study the strength and nature of the intermolecular interactions in these four families by choosing representative examples from each group and computationally evaluating the dependence of the interaction energy on the metal–metal distance. We will do so at the ab initio Hartree–Fock (HF) and second-order Møller–Plesset (MP2) levels of

theory, as well as at the B3LYP density functional level, in order to test the ability of this methodology to handle this type of interactions (see the Computational Methods). At the same time, we will investigate the nature of the interaction by studying the weight of the different components of the interaction energy by means of an intermolecular perturbation analysis using the IMPT method of Hayes and Stone.[76,77] In such a method, the interaction energy is decomposed into five components: exchange–repulsion (E_{er}), electrostatic (E_{el}), polarization (E_{p}), charge transfer (E_{ct}), and dispersion (E_{disp}). The method is perturbative and applies only if the distances between the interacting fragments are long enough. In all cases, we will verify that the sum of the energy components given by the IMPT method matches the total MP2 interaction energy to make sure that we are in the region in which the method is applicable.

The compounds selected for our study were the following: the $[\{Cu(N_2)_2\}_2]^{2+}$ dimer as a representative of the cation··· cation class, $[\{Cu(N_2)Cl\}_2]$ and $[\{Cu(NH_3)Cl\}_2]$ representing the neutral···neutral family, $[Cu(NH_3)_2]^+[CuCl_2]^-$ for the cation···anion (ion pair) group, and $[\{Cu(CH_3)CN\}_2]^{2-}$ for the anion···anion family. We first optimized the geometry of the monomers, which turns out to be linear in all cases, while other optimized geometrical parameters are presented in Table 2. We then computed the interaction energy curves of the dimers at the HF, MP2, and B3LYP levels, placing the monomers in a staggered (perpendicular) orientation, and freezing the monomers at their optimized noninteracting geometries. Two alternative basis sets were used for those curves with the aim of evaluating the possible effect of basis-set truncation: a smaller basis set (identified as LANL2/TZDP+, see the Computational Methods), and a much larger set (identified as SDD/cc, see Computational Methods), which is the (11s9p7d4f)/[9s7p5d3f] basis set of Schwerdtfeger[45,54] that includes three sets of f functions. We finally carried out an IMPT analysis of these interaction energy curves with an all-electron basis set that was previously seen to reproduce the shape of the curves computed with the LANL2/TZDP+ basis set (see the Computational Methods for a description of the all-electron basis sets).

Table 2. Optimized geometry of dicoordinate Cu^I monomers (in all cases the bond angle around Cu is 180° within chemical accuracy) calculated at the MP2 and B3LYP levels. The experimental data gives the range of values found in crystal structures of related compounds.

Compound	Parameter	B3LYP	MP2	Exptl
$[Cu(N_2)_2]^+$	Cu–N	1.924	1.938	
	N–N	1.091	1.113	
$[Cu(N_2)Cl]$	Cu–Cl	1.860	1.826	
	Cu–N	1.985	2.084	
	N–N	1.095	1.117	
$[Cu(NH_3)Cl]$	Cu–Cl	2.098	2.096	2.08–2.16
	Cu–N	1.959	1.933	1.80–1.94
	N–H	1.019	1.021	
	Cu–N–H	112.1	112.6	
	H–N–H	106.7	106.1	
$[Cu(NH_3)_2]^+$	Cu–N	1.929	1.942	1.80–2.11
	N–H	1.023	1.021	
	Cu–N–H	113.3	112.8	
	H–N–H	105.4	106.6	
$[CuCl_2]^-$	Cu-Cl	2.148	2.157	2.00–2.14
$[CuCH_3CN]^-$	Cu–C(CH_3)	1.965	1.951	
	Cu–C(CN)	1.918	1.876	
	C–N	1.163	1.182	
	C–H	1.101	1.102	
	Cu–C–H	112.5	112.8	

Cation···cation dimers: The interaction energy curves for the dimer of a cationic complex, $[\{Cu(N_2)_2\}_2]^{2+}$, computed at the HF, MP2, and B3LYP levels, are shown in Figure 2. Similarly to what was previously reported for the dimer of the neutral complex $[Cu(NH_3)Cl]$,[45,54] the Hartree–Fock curve is repulsive in this case. However, the MP2 energy curve for the cationic dimer is also repulsive by $\approx 80\,kcal\,mol^{-1}$ at 3 Å (although some $5\,kcal\,mol^{-1}$ more stable than the HF curve), whereas it was found to be attractive for the neutral dimer. The B3LYP energy curve is nearly identical to the MP2 one. The quality of the basis set employed has little

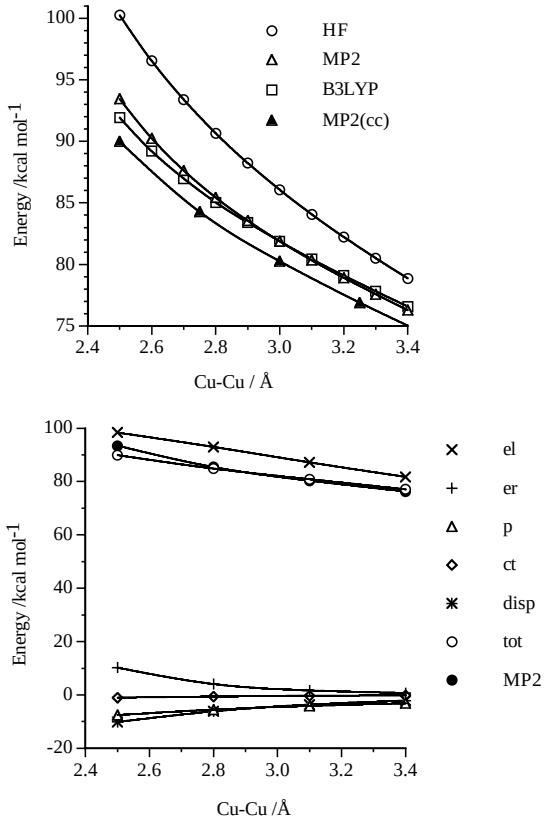

Figure 2. Top: Variation with the Cu···Cu distance of the total interaction energy of the $[\{Cu(N_2)_2\}_2]^{2+}$ dimer computed at the HF, MP2, and B3LYP levels with the LANL2/TZDP+ basis, and at the MP2 level with the SDD/cc basis (labeled MP2(cc)). Bottom: IMPT decomposition of the interaction energy (er = exchange–repulsion, el = electrostatic, p = polarization, ct = charge transfer, tot = sum of the IMPT contributions, MP2 = interaction energy computed with the MP2 method).

effect on the results (Figure 2): the BSSE-corrected curves computed with two basis sets are nearly parallel, the largest set having only slightly lower energies. Therefore, for a dimer of a cationic complex, $[\{Cu(N_2)_2\}_2]^{2+}$, we can safely conclude that the dispersion energy is not large enough to compensate for other repulsive components of the interaction energy and no net stabilizing interaction is found between the monomers. This is in contrast to the findings previously reported for dimers of the neutral complexes, $[Cu(NH_3)Cl]$ and $[Au(PH_3)Cl]$, by Schwerdtfeger[54] and Pyykkö.[43] Therefore, the existence of cation···cation dimers with short Cu–Cu distances in the solid state is a consequence of the presence of counterions and of the corresponding attractive cation···anion interactions, the strength of which overcomes the combined effect of the repulsive cation···cation and anion···anion interactions (this effect has been demonstrated in many ionic crystals by means of ab initio calculations[45,54]).

Table 3. Values of the exchange–repulsion (E_{er}), electrostatic (E_{el}), polarization (E_p), charge-transfer (E_{ct}) and dispersion (E_{disp}) components computed from an IMPT analysis for the indicated dimers. Distances in Å, energies in kcal mol^{-1}. E_{total} is the sum of all components, and E_{MP2} is the MP2 interaction energy computed with the same all-electron basis set and geometry. E_{MP2}(cc) is the MP2 energy computed with the SDD/cc basis set.

Dimer	$r_{Cu\cdots Cu}$	E_{er}	E_{el}	E_p	E_{ct}	E_{disp}	E_{total}	E_{MP2}	E_{MP2}(cc)
$[\{Cu(N_2)_2\}_2]^{2+}$	3.1	1.7	87.2	−4.1	−0.3	−3.1	81.4	80.3	79.9
$[\{Ni(N_2)_2\}_2]$	3.0	31.0	−19.9	−1.8	−1.6	−14.9	−7.2	−7.9	−9.3
$[\{CuCl(NH_3)\}_2]$	3.2	6.0	−3.4	−1.2	−0.5	−4.4	−3.5	−2.2	−3.1
$[Cu(NH_3)_2][CuCl_2]$	2.8	13.6	−80.3	−2.2	−1.0	−7.8	−77.7	−74.2	−82.9
$[\{CuBr(NH_3)\}_2]$	3.4	5.7	−3.7	−1.0	−0.4	−3.7	−3.2	−2.0	–
$[\{CuCl(PH_3)\}_2]$	3.4	3.9	−1.8	−1.1	−0.4	−5.0	−4.3	−2.8	–
$[\{CuBr(PH_3)\}_2]$	3.4	6.2	−3.5	−1.2	−0.5	−5.7	−4.7	−2.9	–
$[\{Cu(CH_3)CN\}_2]^{2-}$	3.4	5.8	62.0	−2.6	−0.8	−5.2	59.2	65.5	63.6
$[\{Au(N_2)_2\}_2]^{2+}$	3.8	1.9	74.0	−3.0	−0.2	−3.1	69.7	71.4	–
$[\{AuCl(NH_3)\}_2]$	3.8	5.3	−3.6	−0.9	−0.3	−3.3	−3.3	−1.7	–

An IMPT analysis of the components of the interaction energy in $[\{Cu(N_2)_2\}_2]^{2+}$ allows us to define which components are important in determining the shape of the curve of Figure 2. The weight of each component is represented in Figure 2 as a function of the metal–metal distance, together with the MP2 interaction energy and the total energy (E_t) obtained by adding all the components of the IMPT calculation (notice the similarity between these two curves). A look at Figure 2 indicates that the electrostatic component is by far the dominant one at all distances. For instance, when the distance between the Cu atoms is 3.1 Å, the electrostatic component (Table 3) is 87.2 kcal mol^{-1}, while the remaining components are all stabilizing and smaller than 5 kcal mol^{-1}, except for a destabilizing exchange–repulsion component. The dispersion term, close to the energy difference between the MP2 and HF interaction energies, is almost 30 times smaller than the electrostatic term. In qualitative terms, what these numbers are telling us is that when two $[Cu(N_2)_2]^{+}$ monomers interact they mostly see each other as positive charges. They also tell us that the Coulombic repulsion between the two cations outweighs the small stabilizing contributions (mostly polarization and dispersion). This conclusion explains why the B3LYP method gives results so close to the MP2 ones, as it is well known that when the interaction energy is dominated by the dispersion term the B3LYP and all other gradient-corrected DFT functionals fail to reproduce the proper shape of the interaction energy curve.[78] We must bear in mind, though, that the repulsions between ions of like charge expected for a dimer in the gas phase are attenuated in the solid state by the Madelung potential provided by the counterions. This has been computationally shown for the case of Au by surrounding a dimer of $[AuL_2]^{+}$ ions with two $[AuCl_2]^{-}$ ions and vice versa.[79]

To further check if the repulsive behavior is associated only with the overall positive charge of the $[Cu(N_2)_2]^{+}$ monomers, we computed the same curve for the neutral isoelectronic $[Ni(N_2)_2]$ monomers. As shown in Figure 3, the HF interaction curve is still repulsive, but the MP2 curve now becomes attractive by almost 10 kcal mol^{-1}, the minimum appearing at ≈2.7 Å, whereby the correlation energy is 16.7 kcal mol^{-1}. Practically the same results are found with the LANL2/TZDP+ and SDD/cc basis sets. The B3LYP

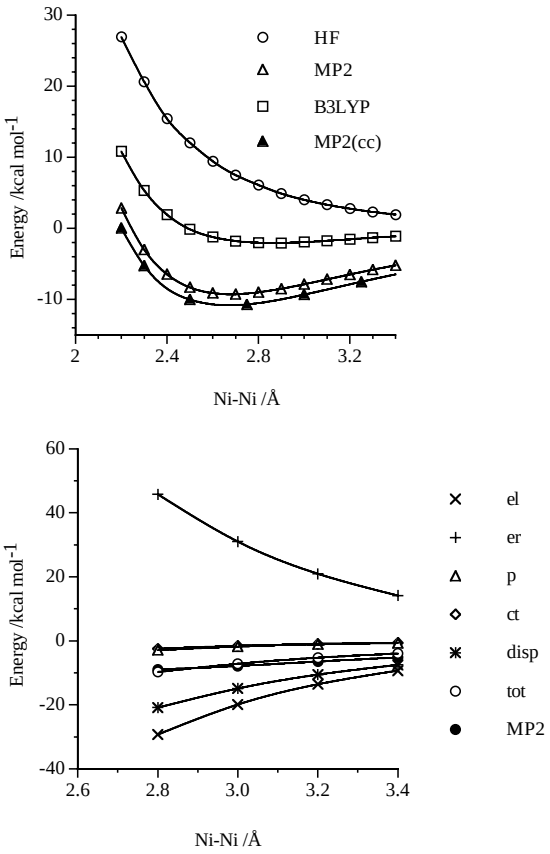

Figure 3. Top: Variation with the Ni···Ni distance of the total interaction energy of the $[\{Ni(N_2)_2\}_2]$ dimer computed at the HF, MP2, and B3LYP levels with the LANL2/TZDP+ basis, and at the MP2 level with the SDD/cc basis (labeled MP2(cc)). Bottom: IMPT decomposition of the interaction energy (er = exchange–repulsion, el = electrostatic, p = polarization, ct = charge transfer, tot = sum of the IMPT contributions, MP2 = interaction energy computed with the MP2 method).

curve is rather less stable, showing a shallow minimum at ≈2.9 Å with a relative energy of −2.0 kcal mol^{-1}. The IMPT decomposition of the interaction energy in the [{Ni(N$_2$)$_2$}$_2$] dimer (Figure 3) clarifies the reasons for the different shapes of the [{Ni(N$_2$)$_2$}$_2$] and [{Cu(N$_2$)$_2$}$_2$]$^{2+}$ interaction curves. A look at Figure 3 or Table 3 shows that the main difference is in the electrostatic component, which is stabilizing (−19.9 kcal mol^{-1}) in the [{Ni(N$_2$)$_2$}$_2$] dimer, but repulsive (87.2 kcal mol^{-1}) in the [{Cu(N$_2$)$_2$}$_2$]$^{2+}$ dimer. The smaller relative weight of the electrostatic component in the interaction energy is the reason for the inferior behavior of the B3LYP curve relative to the MP2 one. The exchange–repulsion term is also larger in the [{Ni(N$_2$)$_2$}$_2$] dimer (31.0 kcal mol^{-1}), but has the same sign as in [{Cu(N$_2$)$_2$}$_2$]$^{2+}$. This term is always repulsive, as it is mostly associated with the repulsive wall caused by the Pauli exclusion principle, which forbids the presence of two electrons in the same region of space. It is partially compensated by a larger dispersion component (−14.9 kcal mol^{-1}, very close to the correlation energy, obtained by subtracting the MP2 and HF total energies). As the remaining terms are much smaller and do not change too much, the overall stability of this dimer comes from the attractive electrostatic and dispersion terms, which together overcome the exchange–repulsion term (note that $E_{er} > E_{disp}$). Consequently, we can safely conclude that: 1) the strong repulsive character of the electrostatic component found in the [{Cu(N$_2$)$_2$}$_2$]$^{2+}$ dimer is associated with the cationic character of each monomer, which dominates over the dispersion term, and 2) when the monomers are neutral, as in the [{Ni(N$_2$)$_2$}$_2$] dimer, the stability of the dimer is associated with the sum of the electrostatic and dispersion terms, and not to the dispersion term alone. Therefore, even in neutral dimers, it is important to take into account the electrostatic term when analyzing the nature of their interaction energy.

Neutral···neutral dimers: The nature of the interaction between neutral [{CuXL}$_2$] dimers was investigated with two model dimers, [{Cu(N$_2$)Cl}$_2$] and [{Cu(NH$_3$)Cl}$_2$]. In the first case, the neutral ligand has no dipole moment, while in the second it has a net moment and emulates better the amines frequently found as ligands. In both models, the anionic chloro ligand compensates the positive charge of the Cu^{I} ion, resulting in neutral monomers. The interaction energies for these two dimers computed at the HF, MP2, and B3LYP levels are shown in Figure 4 for the two basis sets used. The curves for the two compounds show the same qualitative trends, irrespective of the basis set employed: 1) there is a minimum at ≈3.2 Å for both the MP2 and B3LYP levels, although the B3LYP curve is less stable than the MP2 one, and 2) the HF curves show no minimum in the [{Cu(N$_2$)Cl}$_2$] case, but a shallow one (−0.4 kcal mol^{-1}) at very long distances for [{Cu(NH$_3$)Cl}$_2$]. Comparison of the results for the two compounds suggests that it is caused by either a larger dipole moment or by the existence of intermolecular Cl···NH$_3$ interactions.

The IMPT analysis of the interaction energy was carried out only for the [{Cu(NH$_3$)Cl}$_2$] dimer at a Cu···Cu distance of 3.2 Å (Table 3), where the sum of the components nearly

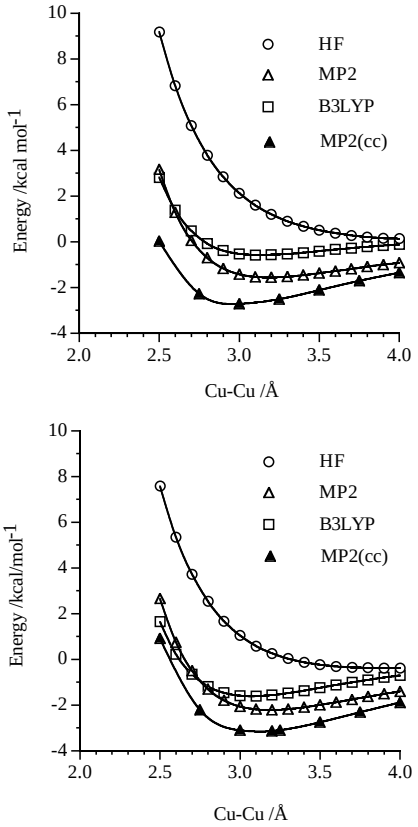

Figure 4. Variation with the Cu···Cu distance of the total interaction energy of the [{Cu(N$_2$)Cl}$_2$] (top) and [{Cu(NH$_3$)Cl}$_2$] (bottom) dimers, computed with the LANL2/TZDP+ basis set with the HF, MP2, and B3LYP methods, and at the MP2 level with the SDD/cc basis set (labeled as MP2(cc) in the figure).

matches the MP2 value. As in the neutral [{Ni(N$_2$)$_2$}$_2$] dimer studied previously, it is the combination of the electrostatic and dispersion components that makes the dimer stable by overcoming the exchange–repulsion term. The IMPT dispersion component (−4.4 kcal mol^{-1}) is, once more, of the order of the MP2–HF total energy difference (correlation energy).

It is worth commenting here on the large difference in the minimum-energy Cu···Cu distances obtained for the [{Cu(NH$_3$)Cl}$_2$] dimer with the BSSE-corrected interaction energy curve (≈3.1 Å, Figure 4 bottom) and with a standard energy optimization (≈2.7 Å[53,54]). One might be tempted to ascribe the much shorter distance to the use of a larger basis set that includes f functions; however, closer inspection of our results indicates that the main difference arises from the basis set superposition error (BSSE). Figure 5 shows the MP2 BSSE-corrected and noncorrected curves, computed with both the LANL2/TZDP+ and SDD/cc basis sets. The standard energy optimizations are carried out without correcting for the BSSE, eventually applying such a correction for the minimum energy geometry to evaluate the interaction energy. Thus, standard optimization gives an optimum Cu···Cu distance close to 2.7 Å with the LANL2/TZDP+ basis set, and close to 2.9 Å with the larger SDD/cc basis set. When the BSSE is corrected at each Cu···Cu distance, the optimum is ≈3.1 Å with both basis sets (this would be the value obtained if the geometry optimization had been

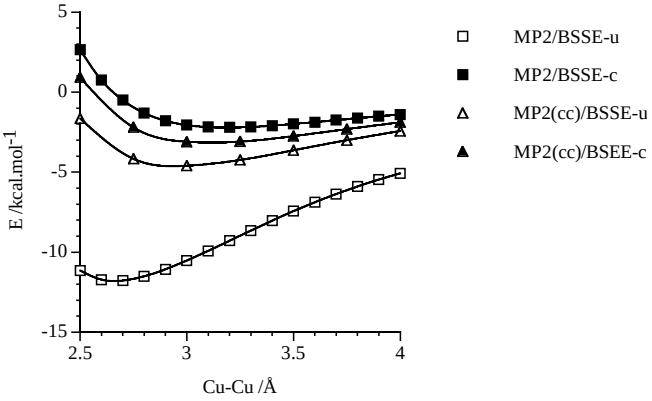

Figure 5. Variation with the Cu···Cu distance of the BSSE-uncorrected and BSSE-corrected MP2 interaction energy of the $[\{Cu(NH_3)Cl\}_2]$ dimer, computed with the LANL2/TZDP+ basis set (labeled as MP2/BSSE-u and MP2/BSSE-c) and the SDD/cc basis set (labeled as MP2(cc)/BSSE-u and MP2(cc)/BSSE-c in the figure).

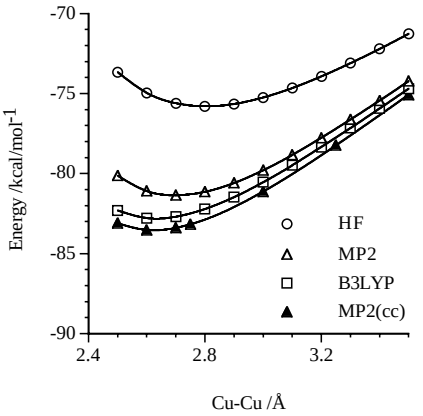

Figure 6. Variation with the Cu···Cu distance of the total energy of interaction between the $[Cu(NH_3)_2]^+$ and $[CuCl_2]^-$ ionic complexes, computed with the LANL2/TZDP+ basis set with the HF, MP2, and B3LYP methods, and at the MP2 level with the SDD/cc basis set (labeled as MP2(cc) in the figure).

performed on the BSSE-corrected potential-energy surface). Therefore, we can conclude that the larger distances found here, relative to the optimized values reported previously by ourselves[53] and by Schwerdtfeger,[54] are not strictly the consequence of using f functions in the basis set, but to the intrinsic properties of the standard optimization procedure that works with BSSE-uncorrected values. From Figure 5, it is clear that inclusion of f functions in the basis set diminishes the BSSE. However, the BSSE-corrected curve computed with the f-containing basis set is similar to that obtained with the smaller basis set (compare the two upper curves in Figure 5). Optimizing the N-Cu-Cl angle of monomers in the dimer is not expected to modify this conclusion, since the optimum value of this angle is very close to 180°.[53] At this point, we must also stress that the BSSE-corrected curves are quite shallow and less than 1 kcal mol^{-1} is involved in changes of the Cu···Cu distance as large as 0.4 Å. This is in full agreement with the variability of such parameters found in the experimental structures (Table 1).

Cation···anion pairs: The nature of the interactions in these ion pairs can be studied with the $[Cu(NH_3)_2]^+[CuCl_2]^-$ case. At the optimum geometry of the isolated ions (Table 2), the dependence of the interaction energy on the Cu···Cu distance for the staggered conformation of the dimer is that depicted in Figure 6. The HF, MP2, and B3LYP curves all show minima, the last two curves being very close to each other with minima at $\approx$2.7 Å, just 0.1 Å shorter than the shortest experimental one (Table 1). The MP2 curves computed with the LANL2/TZDP+ and SDD/cc basis sets are parallel, thus giving the same qualitative information (Figure 6). It must be mentioned, however, that only two experimental structures have been found and comparison with our calculated data is not straightforward, given the different neutral ligands present in the experimental compounds. The IMPT analysis of the interaction energy (carried out at 2.8 Å, where the sum of the IMPT components is still close to the MP2 interaction energy, see Table 3) shows that the dominant component is the electrostatic one, strongly attractive in this case and approximately seven times larger than the exchange–repulsion component. The dispersion term is third in magnitude (-7.8 kcal mol^{-1}), well above the polarization and charge-transfer terms, and of the order of the MP2–HF energy difference. Thus, in qualitative terms, the present IMPT analysis suggests that the $[Cu(NH_3)_2]^+\cdots[CuCl_2]^-$ interaction can be essentially described as an electrostatic attraction between a positive and a negative charge. This conclusion, which emphasizes the importance of the electrostatic component in dimers with a short Cu–Cu distance, has been already pointed out for another Cu^{I} ion pair by Poblet and Bénard.[80]

Anion···anion dimers: We have studied the nature of the anion···anion interactions on the basis of the $[\{Cu(CH_3)CN\}_2]^{2-}$ dimer as a model, with the monomers at their optimized geometry (Table 2). The HF, MP2, and B3LYP interaction energy curves all exhibit the same features (Figure 7), clearly showing the repulsive nature of the intermolecular interaction, irrespective of the computational

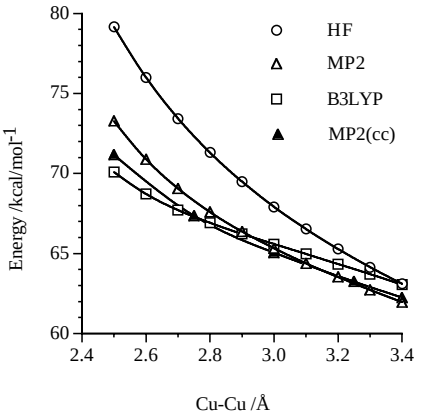

Figure 7. Interaction energy between two anionic $[Cu(CH_3)CN]^-$ complexes as a function of the Cu···Cu distance, calculated with the LANL2/TZDP+ basis set and the HF, MP2, and B3LYP methods, and at the MP2 level with the SDD/cc basis set (labeled as MP2(cc) in the figure).

method used. The IMPT analysis of the components of the interaction energy (Table 3) shows that the dominant term is by far the electrostatic one, which is repulsive and represents 95% of the interaction energy. Thus, the interaction between the two anionic monomers can be essentially described as the repulsion between two negative charges.

Such a result is in sharp contrast with the fact that the $[\{Cu(t\text{Bu})CN\}_2]^{2-}$ dimer has the shortest Cu···Cu contact (Table 1). Calculations on a dimer with an experimental structure in which the *t*Bu groups have been replaced by methyl groups consistently indicate that interaction between the two anionic monomers is destabilizing (by 66.2 kcal mol^{-1} at the MP2 level with BSSE correction). However, if the Li^+ ions closest to the cyano groups are included in the calculations (Figure 8, right), the Li_2^{2+} $[\{Cu(CH_3)CN\}_2]^{2-}$ aggregate is stable towards its dissociation

Figure 8. Left: part of the crystal structure of Li[Cu(*t*Bu)CN] showing the Cu···Cu contacts in dimers and the connection of neighboring dimers through Li^+ ions. Right: neutral dimer incorporating one Li^+ ion per copper atom discussed in the text.

into two cationic and two anionic fragments by 230 kcal mol^{-1}, an order of magnitude similar to that found in many other ionic crystals for similar aggregates. (see, for example, refs. [81, 82]).

Other dimers: We have extended our IMPT analysis to other Cu···Cu and to two Au···Au dimers to test the validity of the above conclusions (Table 3). In all cases, the results are consistent with those discussed above: the electrostatic term being the dominant energy contribution when the interacting species are charged, while both the electrostatic and dispersion components are of nearly equal importance for dimers of neutral species.

General picture of the Cu···Cu interactions The results for the various dimers studied up to now can be summarized as follows:

1) The sum of the components of the IMPT analysis differs from the MP2 interaction energies by less than 2 kcal mol^{-1} in practically all cases.
2) There is a parallelism between the net interaction energy and the electrostatic term, as a consequence, interactions between cationic monomers are strongly repulsive, whereas those between ions of opposite charge are strongly attractive.
3) Even for dimers of neutral complexes, the Coulombic interaction is as important or even larger than the dispersion component.
4) The dispersion term is always attractive; however, in most cases, it is not large enough to compensate for the exchange repulsion.
5) The net character of the interaction is always properly reproduced by the combination of the electrostatic and dispersion terms. This point is well illustrated in Figure 9, in which the calculated MP2 interaction energy

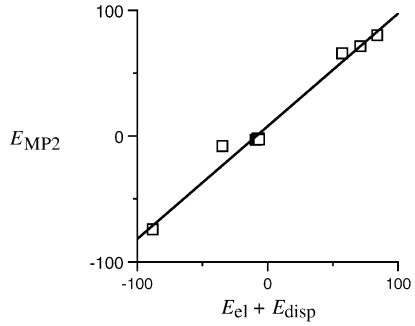

Figure 9. Relationship between the sum of the Coulomb and dispersion terms of the IMPT analysis for several bimolecular aggregates (Table 3) and the MP2 interaction energy. All energies are in kcal mol^{-1}.

for all compounds in Table 3 presents an excellent correlation with the sum of the electrostatic and dispersion components.
6) The polarization and charge-transfer components are always attractive, but smaller than the dispersion term.
7) The main conclusion of the combined MP2 and IMPT analysis presented here is that not all short Cu···Cu interactions are similar in nature. The magnitude and relative importance of the components of the interaction energy change strongly with the charge of the fragments, thus making necessary to classify these interactions into subgroups according to the charge of the fragments. Since interactions between charged molecules of the same sign are repulsive, their dimers can only exist in condensed phases owing to the stabilizing Madelung potential of counterions, not to the attractive nature of the Cu···Cu interactions. Alternatively, an aggregate of particles of the same sign is possible in solution, because of the attractive effect of the solvent, which may be strong enough to create a stable aggregate.[83]
8) The B3LYP DFT functional reproduces the MP2 curve of the Cu···Cu compounds studied here when the electrostatic component is the dominant one in the interaction energy, but fails in systems where the dispersion component is important.

The previous energetic results are consistent with those reported by Poblet et al. for a specific ion pair,[80] as well as with those from a previous LMP2 analysis for neutral dimers[46,47] (with regard to the LMP2 work, we should note that, although some terms have the same name as in the present IMPT study, the two methods use different approaches and such terms do not always represent the same physical effect). The combination of different contributions and their dependence on the intermolecular distance (see, for example, Figure 2) may explain why no correlation has been found between the experimental distance and the electronegativity of the X ligand in the $[\{AuX(PMe_2Ph)\}_2]$ and

$[\{AuX(CNtBu)\}_2]$ series, as reported by Schmidbaur et al.[4] When varying the ligands in $[\{CuX(EH_3)\}_2]$ (X = Cl, Br; E = N, P), we observe that the dispersion term becomes more stabilizing as the electronegativity of the donor atoms is decreased (Table 3). The exchange–repulsion and the Coulomb terms are also sensitive to the nature of the ligands, whereas the charge-transfer and polarization terms are practically unchanged. It must be noted also that in previous theoretical studies the interacting monomers were forced to remain perpendicular to each other to disregard the dipolar electrostatic interaction, whereas the present results suggest that these interactions are still responsible for a large part of the intermolecular interaction energy.

We checked that the previous conclusions are not dependent on the method or basis set employed. The independence from the method was evaluated by checking the convergence of the MP2 results against MP3 and MP4 values, and also by computing the CCSD(T) value on the $[\{Cu(N_2)_2\}_2]^{2+}$, $[\{Cu(NH_3)Cl\}_2]$, and $[Cu(NH_3)_2]^{+}[CuCl_2]^{-}$ dimers, taken as prototype of dicationic, neutral, and cationic–anionic dimers, respectively. All these methods give similar interaction energies. The MP*n* series presents small oscillations, and the CCSD(T) interaction energy is slightly more stabilizing than the MP2 one (by 0.7, 0.5, and 0.8 kcal mol^{-1}, on each of the above dimers). The absolute value of the MP2 interaction energy differs from the CCSD(T) energy by 0.5 kcal mol^{-1} in average). Furthermore, the MP2 method presents the smallest difference with the CCSD(T) among those computed here. We also tested the impact of the use of more extended basis sets by recomputing the MP2 interaction energy of the dimer of $[Cu(NH_3)Cl]$ with the correlation-consistent basis set of Hermann et al.,[54] designed to minimize the basis set superposition error (BSSE). The BSSE-corrected values obtained at the LANL2DZ/TZP+ level differ by less than 1 kcal mol^{-1} from those obtained with the correlation-consistent basis set of Hermann, and both have the minimum of their curves at similar distances. The similarity of these results suggests that the LANL2DZ/TZP+ basis set is flexible enough to evaluate with accuracy the interaction energy in these complexes,[84–86] provided the results are corrected for the BSSE. Studies on ionic systems indicate that the BSSE of the MP2 calculations is close to that obtained within the Hartree–Fock method, that is, much smaller than that found in neutral dimers.[87]

The previous computations have evaluated the interaction energy between Cu^{I} dicoordinate complexes oriented in an orthogonal conformation ($\tau = 90°$, see **6**) to minimize the interaction between the ligands,[47,54] although other types of dimers can be considered.[53] However, one question arises here, even for a perpendicular orientation: how much of the interaction energy of the dimer can be attributed *solely* to the interaction between the copper atoms themselves? A previous study of two Cu complexes has shown that only 18% of the dispersion component can be associated with the Cu···Cu interaction.[47] The present study has shown that the energy of interaction between monomers is dominated by a combination of the electrostatic and dispersion terms. A simple electrostatic point-charge model (Table 4) shows that the overall electrostatic energy is the result of a complicated interplay between the Cu···Cu, Cu···ligand, and ligand···ligand interactions, which do not always have the same sign, the Cu···Cu interaction being not even the dominant one. Therefore, although a Bader analysis of the electron density (see Figure 10) at the crystal structure geometry shows the presence of a (3, −1) bond-critical point linking the Cu atoms, which suggests the existence of Cu···Cu bonding between the fragments, one can wonder if it is appropriate to talk about Cu···Cu bonds in this situation, because the use of this concept could imply that we are associating the energy of the dimer to the Cu···Cu bonding interaction, as has been done up to now. Can we still talk about Cu···Cu bonds in these complexes?

Table 4. Qualitative analysis of the electrostatic energy in terms of the interactions between the Cu atoms (Cu···Cu), the Cu atoms and the ligands L (Cu···L, where L includes both ligands, irrespective of their type), and the interactions between the ligands (L···L). The three components have been computed on the basis of a simple charge–charge model, whereby the charges on each atom have been taken from a Mulliken population analysis of the isolated monomers (HF method, LAND2DZ+2P/TZ+P basis set). The numbers are only indicative of trends, though their sum is close to the electrostatic component computed in the IMPT analysis, E_{el}(IMPT), and they are included in the last column for comparison. All values are in kcal mol^{-1}.

	Cu···Cu	Cu···L	L···L	Sum	E_{el}(IMPT)
$[Cu(N_2)_2]^{+}$	46.2	28.4	5.2	79.9	81.8
$[CuCl(NH_3)]^{+}$	6.9	−14.2	7.3	0.0	−2.2
$[Cu(NH_3)_2]^{+}[CuCl_2]^{-}$	23.9	−70.1	−22.2	−68.4	−69.6
$[Cu(CH_3)(CN)]^{-}$	13.1	−83.1	135.8	65.8	62.0
$[Ni(N_2)_2]$	0.3	−0.4	0.2	0.1	−9.3

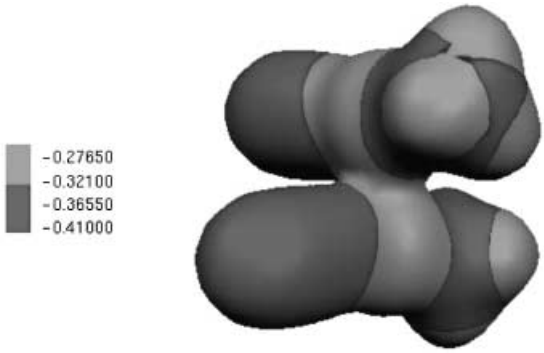

Figure 10. Electron-density map of $[\{Cu(CH_3)CN\}_2]^{2-}$ (0.05 a.u. isosurface) on which the electrostatic energy map is projected (see left bar for gray scale code). The (3, −1) bond-critical point is placed in the region where the densities of the two fragments overlap, and links the two Cu atoms.

A proper answer to the previous question requires a revision of the concept of a bond. According to Pauling, "there is a chemical bond between two atoms or groups of atoms in case that the forces acting between them are such as to

lead to the formation of an aggregate with sufficient stability to make it convenient for the chemist to consider it as an independent molecular species".[88] Clearly, the results reported here indicate that the bimolecular aggregates formed by two d^{10} dicoordinate complexes may correspond to one of two cases, based on energetic criteria: 1) stable $CuX^1Y^1\cdots CuX^2Y^2$ fragments, formed by the neutral···neutral and ionic pair cases and 2) unstable $CuX^1Y^1\cdots CuX^2Y^2$ aggregates of the anion···anion and cation···cation types. The first case is consistent with Pauling's definition of a chemical bond. Thus, although the stability of the bimolecular aggregate is mostly caused by Cu···ligand interactions, we propose that these can be still termed *Cu···Cu bonds*, even if most of the bonding does not actually come from interaction between the Cu atoms. Such a naming convention is usually adopted for other intermolecular bonding situations for which the interaction between the atoms involved in the *bond* is not always the dominant one. For example, in a hydrogen bond between water molecules, the electrostatic interaction between the OH···O atoms is not equal to the total electrostatic energy between the fragments, as computed in a fourth-order distributed multipole analysis.

When the fragments are not energetically stable, following Pauling's definition, one should not talk about Cu···Cu bonds. These Cu···Cu dimers are found in larger aggregates, owing to forces external to the dimer, for example, the presence of counterions. This is indeed what happens within ionic crystals in which $CuXY^{n+/n-}$ fragments are present. Thus, as previously discussed, the $[\{Cu(CH_3)CN\}_2]^{2-}$ dimer is energetically unstable when isolated, but becomes stable when two Li^+ ions are added at the geometry found in the crystal structure of the related experimental *t*Bu complex. Consequently, in the $[\{Cu(CH_3)CN\}_2]^{2-}\cdots Li_2^{2+}$ aggregate it is the $Li^+\cdots[Cu(CH_3)CN]^-$ interactions that force the two anions to approach each other, even at shorter distances than those found in the neutral CuXY fragments, despite the strongly repulsive nature of the anion···anion interaction. When the cation···anion interaction brings the two anions close to each other, their orbitals are forced to interact and the same orbital diagrams (e.g., **13** and **14**, respectively) and electronic properties (e.g., luminescence) of the neutral··· neutral case apply. A related situation is found for a "dimer" of TCNE, which behaves as if an intermolecular C–C bond exists, even though calculations show the monomer···monomer interaction to be repulsive in the gas phase.[89–91] Therefore, although they exhibit many of the properties expected for a bond, we cannot appropriately refer to the interaction present between $CuXY^{n+/n-}$ fragments as Cu···Cu bonds. One could call them *counterion-mediated Cu···Cu bonds*, thus stressing the supramolecular origin of the bond. These counterion-mediated Cu···Cu bonds have similar electronic properties to the Cu···Cu bonds and, consequently, can go unnoticed unless an analysis of the energetic components between all the fragments is performed. Thus, for instance, in addition to the previously mentioned similarity in the orbital interaction diagram, a $(3,-1)$ bond-critical point between the Cu atoms is found in the $[\{Cu(CH_3)CN\}_2]^{2-}\cdots Li_2^{2+}$ aggregate (Figure S1 in the Supporting Information), and a critical point is also present in a $[\{Cu(CH_3)CN\}_2]^{2-}$ dimer placed at the same geometry found in the previous aggregate for the anions (Figure 10).

Conclusion

By performing HF and MP2 computations on model systems representative of the situations found in crystal structures, the nature of the interactions between dicoordinate monomers of Cu^I is found to be strongly dependent on their net charges. An IMPT analysis of the interaction energy reveals that the electrostatic component of the interaction energy is the leading term in the interaction when the dimers are charged, while in all cases it is a combination of the electrostatic component and the dispersion component that reproduces the distance dependence of the total interaction energy. These results are consistent with previous indications that the Coulombic contribution was important for the interaction between ionic complexes (see, for example, the work of Poblet and Bénard[80]). B3LYP computations roughly reproduce the shape and stability of the MP2 curves when the electrostatic component in the interaction energy is important.

Consistent with that electrostatic dispersion nature, the $Cu^I\cdots Cu^I$ interactions between monomers of the same charge are found to be energetically unstable. As energetic stability is an essential condition for the presence of a bond between two fragments, we cannot speak of the existence of any bond between the fragments in such a case. Our analysis shows that the presence of anion···anion or cation···cation bimolecular aggregates is caused by the presence of the counterions: the cation···anion interaction largely outweighs the cation···cation plus anion···anion interactions, thus forcing the anions to approach each other. The fact that the two anions stay in close proximity allows for the overlap of the orbitals of the two fragments, thus triggering in these charged bimolecular aggregates the same orbital interaction and energetic splitting normally found when two fragments interact to produce bonds.

Energetically stable dimers exhibiting $Cu^I\cdots Cu^I$ interactions have been found when the two monomers involved in the interaction are neutral or hold opposite charges, thus allowing us to speak of a bond between the fragments of the bimolecular aggregate. A proper analysis of the interaction energy in this case indicates that only a small part of that energy results from Cu···Cu interactions, while a large component results from Cu···ligand interactions. Despite this fact, we propose to keep talking about the presence of Cu···Cu bonds in these aggregates, but keeping in mind the actual energetic structure of this bond.

Computational Methods

The structural data were obtained through systematic searches of the Cambridge Structural Database[10] (version 5.23). The search was conducted for transition-metal compounds of general formula MXY in which M was imposed to have a total coordination number of two, and X and Y were allowed to be any atom of Groups 14–17. Only structures with no disorder and agreement factors $R<10\,\%$ were accepted as hits. Such

searches were restricted to those compounds in which only one intermolecular M···M contact per metal atom within the distance specified in the text for each metal.

All ab initio calculations were performed with the Gaussian 98 suite of programs. The electron correlation was introduced through the Møller–Plesset perturbation approach to second order (MP2).[31] Two types of computations were performed to obtain the interaction energy curves: one described Cu with LANL2 pseudopotentials and a basis set of triple-ζ quality to which polarization and diffuse functions were added (denoted LANL2/TZDP+), and another in which Cu was described with the SDD pseudopotentials combined with a (11s9p7d4f)/[9s7p5d3f] basis set (denoted SDD/cc). The LANL2/TZDP+ basis sets for Cu and Ni atoms were obtained by decontracting the three components of the LANL2DZ basis set, and then adding two sets of p-polarization functions (exponents 0.053 and 0.164 on Cu, 0.049 and 0.153 on Ni) and one set of s, p, and d diffuse functions (exponents 0.0396, 0.024, and 0.03102 on each set for the two metals). The LANL2/TZDP+ basis set for the remaining atoms was obtained by taking the LANL2DZ basis set and adding two d functions on all atoms except the hydrogens (exponents: 0.412 and 1.986 on N, 0.153 and 0.537 on P, 0.288 and 1.335 on C, 0.227 and 0.797 on Cl, 0.162 and 0.548 on Br). The SDD/cc basis set on Cu was that with the (11 s9p7d4f)/[9 s7p5d3f] valence basis set computed by Schwerdtfeger,[54] in which the inner electrons were described by the SDD pseudopotentials, while the H atoms were described by cc-pVDZ,[92] the C, N, O, Cl atoms were described by the cc-pVTZ,[92] and the Ni atom by the SDD pseudopotentials and the valence basis set of Dolg et al.[93]

All-electron basis sets were used for the IMPT analysis, because the IMPT implementation available to us does not work with pseudopotential cores. The all-electron basis set for each dimer was selected in such a way that it reproduces the shape of the interaction energy curve of the dimer computed with the LANL2/TZDP+ basis set and with pseudopotentials; it differs from dimer to dimer. For the all Cu-containing dimers, the all-electron basis set was built by taking for Cu the pVDZ basis set of Ahlrichs[94] supplemented by a diffuse d function (exponent 0.03102) and a p-polarization function (exponent 0.052), and the 3-21G basis set for the remaining atoms (this gives similar curves to the LANL2/TZDP+ basis set at any level, though the all-electron curves are ≈ 5 kcal mol^{-1} more stable). In the neutral $[Ni(N_2)_2]$ monomers, we used the pVDZ of Ahlrichs,[94] adding a p polarization function (exponent 0.049) and a diffuse d function (exponent 0.03102), while we used a 3-21G basis set at the N atoms. The attractive character of the interaction between $[Ni(N_2)_2]$ monomers at the MP2 level, which becomes repulsive at the HF level, was also found in the all-electron basis set of TZDP character.

In the dimer calculations, the two monomers were always oriented in a staggered conformation ($\tau = 90°$, **6**) to minimize the ligand···ligand interactions because we were interested in the defining the nature of the Cu···Cu interactions in these dimers. The geometries of the monomers were kept frozen when computing the interaction energy curve at the MP2 and B3LYP levels and during the IMPT analysis of these curves. In all cases, the interaction energy was corrected for the possible basis set superposition error (BSSE) by means of the full counterpoise method,[95] except when explicitly stated for comparative purposes.

Acknowledgments

Financial support of this work was provided by the Ministerio de Ciencia y Tecnología (projects BQU2002–04033-C02-01 and BQU2002-04587-C02-02) and by Comissionat per a Universitats i Recerca (Generalitat de Catalunya) through grant 2001SGR-0044. The computing resources at the Centre de Supercomputació de Catalunya (CESCA) and Centre Europeu de Paralelisme de Barcelona (CEPBA) were made available in part through a grant of Fundació Catalana per a la Recerca (FCR) and Universitat de Barcelona. The authors thank the anonymous referees for their helpful criticism and suggestions.

[1] M. Jansen, *Angew. Chem.* **1987**, *99*, 1136; *Angew. Chem. Int. Ed. Engl.* **1987**, *26*, 1098.
[2] P. Pyykkö, *Chem. Rev.* **1997**, *97*, 597.
[3] A. Grohmann, H. Schmidbaur, in *Comprehensive Organometallic Chemistry II, Vol. 3* (Ed.: J. L. Wardell), Pergamon, Oxford, **1995**, p. 1.
[4] T. Mathieson, A. Schier, H. Schmidbaur, *J. Chem. Soc. Dalton Trans.* **2000**, 3881.
[5] H. Schmidbaur, *Gold Bull.* **1990**, *23*, 11.
[6] A. Byström, L. Evers, *Acta Chem. Scand.* **1950**, *4*, 613.
[7] M. Jansen, M. Bortz, K. Heiderbrecht, *J. Less-Common Met.* **1990**, *161*, 175.
[8] F. Scherbaum, A. Grohmann, B. Huber, C. Krüger, H. Schmidbaur, *Angew. Chem.* **1988**, *100*, 1602; *Angew. Chem. Int. Ed. Engl.* **1988**, *27*, 1544.
[9] J. Vicente, M. T. Chicote, M. C. Lagunas, *Inorg. Chem.* **1993**, *32*, 3748.
[10] J. Vicente, M.-T. Chicote, I. Saura-Llamas, M.-C. Lagunas, M. C. Ramírez de Arellano, P. González-Herrero, M.-D. Abrisqueta, R. Guerrero, in *Metal Clusters in Chemistry, Vol. 1* (Eds.: P. Braunstein, L. A. Oro, P. R. Raithby), Wiley-VCH, New York, **1999**, p. 493.
[11] O. Crespo, M. C. Gimeno, A. Laguna, in *Metal Clusters in Chemistry, Vol. 1* (Eds.: P. Braunstein, L. A. Oro, P. R. Raithby), Wiley-VCH, New York, **1999**, p. 477.
[12] M. Freytag, P. G. Jones, *Chem. Commun.* **2000**, 277.
[13] B. Ahrens, P. G. Jones, A. K. Fischer, *Eur. J. Inorg. Chem.* **1999**, 1103.
[14] M. John, C. Auel, C. Behrens, M. Marsch, K. Harms, F. Basolo, R. M. Gschwind, P. R. Rajamohanan, G. Boche, *Chem. Eur. J.* **2000**, *6*, 3060.
[15] L. Manojlovic-Muir, K. W. Muir, M. C. Grossel, M. P. Brown, C. D. Nelson, A. Yavari, E. Kallas, R. P. Moulding, K. R. Seddon, *J. Chem. Soc. Dalton Trans.* **1986**, 1955.
[16] W. Bensch, M. Prelati, W. Ludwig, *J. Chem. Soc. Chem. Commun.* **1986**, 1762.
[17] O. W. Howarth, G. G. Morgan, V. McKee, J. Nelson, *J. Chem. Soc. Dalton Trans.* **1999**, 2097.
[18] J. Zank, A. Schier, H. Schmidbaur, *J. Chem. Soc. Dalton Trans.* **1998**, 415.
[19] C.-M. Che, Z. Mao, V. M. Miskowski, M.-C. Tse, C.-K. Chan, K.-K. Cheung, D. L. Phillips, K.-H. Leung, *Angew. Chem.* **2000**, *112*, 4250; *Angew. Chem. Int. Ed.* **2000**, *39*, 4084.
[20] M. Wachhold, M. G. Kanatzidis, *Inorg. Chem.* **1999**, *38*, 4178.
[21] M. S. Lüth, E. Freisinger, F. Glahe, B. Lippert, *Inorg. Chem.* **1998**, *37*, 5044.
[22] A. A. Palacios, G. Aullón, P. Alemany, S. Alvarez, *Inorg. Chem.* **2000**, *39*, 3166.
[23] N. L. Pickett, O. Just, D. G. VanDerveer, W. S. Rees, Jr., *Acta Crystallogr.* **2000**, *56*, 412.
[24] D. M. Blake, C. J. Nyman, *J. Am. Chem. Soc.* **1970**, *92*, 5359.
[25] M. Bénard, U. Bodensieck, P. Braunstein, M. Knorr, M. Strampfer, C. Strohmann, *Angew. Chem.* **1997**, *109*, 2890; *Angew. Chem. Int. Ed. Engl.* **1997**, *36*, 2758.
[26] S. Wang, J. P. Fackler, Jr., *Organometallics* **1988**, *7*, 2415.
[27] M. Contel, J. Garrido, M. C. Gimeno, M. Laguna, *J. Chem. Soc. Dalton Trans.* **1998**, 1083.
[28] R. E. Rundle, *J. Am. Chem. Soc.* **1954**, *76*, 3101.
[29] O. Crespo, A. Laguna, E. J. Fernández, J. M. López-de-Luzuriaga, P. G. Jones, M. Teichert, M. Monge, P. Pyykkö, N. Runeberg, M. Schütz, H.-J. Werner, *Inorg. Chem.* **2000**, *39*, 4786.
[30] K. Yoon, G. Parkin, *Polyhedron* **1995**, *14*, 811.
[31] H.-R. C. Jaw, M. M. Savas, R. D. Rogers, W. R. Mason, *Inorg. Chem.* **1989**, *28*, 1028.
[32] N. E. Brese, M. O'Keeffe, B. L. Ramakrishna, R. B. v. Dreele, *J. Solid State Chem.* **1990**, *89*, 184.
[33] K.-H. Leung, D. L. Phillips, M.-C. Tse, C.-M. Che, V. M. Miskowski, *J. Am. Chem. Soc.* **1999**, *121*, 4799.
[34] M. A. Omary, T. R. Webb, Z. Assefa, G. E. Shankle, *Inorg. Chem.* **1998**, *37*, 1380.
[35] D. E. Harwell, M. D. Mortimer, C. B. Knobler, F. A. L. Anet, M. F. Hawthorne, *J. Am. Chem. Soc.* **1996**, *118*, 2679.
[36] J. Zank, A. Schier, H. Schmidbaur, *J. Chem. Soc. Dalton Trans.* **1998**, 323.

[37] H. Schmidbaur, W. Graf, G. Müller, *Angew. Chem.* **1988**, *100*, 439; *Angew. Chem. Int. Ed. Engl.* **1988**, *27*, 417.
[38] R. Narayanaswamy, M. A. Young, E. Parkhurst, M. Ouellette, M. E. Kerr, D. M. Ho, R. C. Elder, A. E. Bruce, M. R. M. Bruce, *Inorg. Chem.* **1993**, *32*, 2506.
[39] S. S. Tang, C.-P. Chang, I. J. B. Lin, L.-S. Liou, J.-C. Wang, *Inorg. Chem.* **1997**, *36*, 2294.
[40] P. K. Mehrotra, R. Hoffmann, *Inorg. Chem.* **1978**, *17*, 2187.
[41] Y. Jiang, S. Alvarez, R. Hoffmann, *Inorg. Chem.* **1985**, *24*, 749.
[42] J. Li, P. Pyykkö, *Chem. Phys. Lett.* **1992**, *197*, 586.
[43] P. Pyykkö, Y. Zhao, *Angew. Chem.* **1991**, *103*, 622; *Angew. Chem. Int. Ed. Engl.* **1991**, *30*, 604.
[44] P. Pyykkö, N. Runeberg, F. Mendizabal, *Chem. Eur. J.* **1997**, *3*, 1451.
[45] P. Pyykkö, F. Mendizabal, *Chem. Eur. J.* **1997**, *3*, 1458.
[46] N. Runeberg, M. Schütz, H.-J. Werner, *J. Chem. Phys.* **1999**, *110*, 7210.
[47] L. Magnko, M. Schweizer, G. Rauhut, M. Schütz, H. Stoll, H.-J. Werner, *Phys. Chem. Chem. Phys.* **2002**, *4*, 1006.
[48] L. F. Veiros, M. J. Calhorda, *J. Organomet. Chem.* **1996**, *510*, 71.
[49] A. Schäfer, R. Ahlrichs, *J. Am. Chem. Soc.* **1994**, *116*, 10692.
[50] A. Schäfer, C. Huber, J. Gauss, R. Ahlrichs, *Theor. Chim. Acta* **1993**, *87*, 29.
[51] C. Kölmel, R. Ahlrichs, *J. Phys. Chem.* **1990**, *94*, 5536.
[52] X.-Y. Liu, F. Mota, P. Alemany, J. J. Novoa, S. Alvarez, *Chem. Commun.* **1998**, 1149.
[53] M. A. Carvajal, X.-Y. Liu, P. Alemany, J. J. Novoa, S. Alvarez, *Int. J. Quantum Chem.* **2002**, *86*, 100.
[54] H. L. Hermann, G. Boche, P. Schwerdtfeger, *Chem. Eur. J.* **2001**, *7*, 5333.
[55] E. Ruiz, S. Alvarez, P. Alemany, R. A. Evarestov, *Phys. Rev. B* **1997**, *56*, 7189.
[56] A. Buljan, P. Alemany, E. Ruiz, *J. Phys. Chem. B* **1999**, *103*, 8060.
[57] M. A. Romero, J. M. Salas, M. Quirós, M. P. Sánchez, J. Molina, J. El Bahraoui, R. Faure, *J. Mol. Struct.* **1995**, *354*, 189.
[58] J. M. Forward, J. P. Fackler, Jr., Z. Assefa, in *Optoelectronic Properties of Inorganic Compounds* (Eds.: M. Roundhill, J. P. Fackler, Jr.), Plenum, **1998**.
[59] G. A. Bowmaker, in *Gold: Progress in Chemistry, Biochemistry and Technology* (Ed.: H. Schmidbaur), J. Wiley, New York, **1999**, p. 842.
[60] R. F. Ziolo, S. Lipton, Z. Dori, *J. Chem. Soc. Chem. Commun.* **1970**, 1124.
[61] W. B. Jones, J. Yuan, R. Narayanaswamy, M. A. Young, R. C. Elder, A. E. Bruce, M. R. M. Bruce, *Inorg. Chem.* **1995**, *34*, 1996.
[62] C. King, M. N. I. Khan, R. J. Staples, J. P. Fackler, Jr., *Inorg. Chem.* **1992**, *31*, 3236.
[63] W. E. van Zyl, J. M. López de Luzuriaga, J. P. Fackler, Jr., *J. Mol. Struct.* **2000**, *516*, 99.
[64] M. A. Rawashdeh-Omary, M. A. Omary, H. H. Patterson, *J. Am. Chem. Soc.* **2000**, *122*, 10371.
[65] J. T. Markert, N. Blom, G. Roper, A. D. Perregaux, N. Nagasundaram, M. R. Corson, A. Ludi, J. K. Nagle, H. H. Patterson, *Chem. Phys. Lett.* **1985**, *118*, 258.
[66] N. Nagasundaram, G. Roper, J. Biscoe, J. W. Chai, H. H. Patterson, N. Blom, A. Ludi, *Inorg. Chem.* **1986**, *25*, 2947.
[67] V. W.-W. Yam, C.-L. Chan, C.-K. Li, K. M.-C. Wong, *Coord. Chem. Rev.* **2001**, *216–217*, 173.
[68] V. W.-W. Yam, C.-K. Li, C.-L. Chan, *Angew. Chem.* **1991**, *103*, 622; *Angew. Chem. Int. Ed.* **1998**, *37*, 2857.
[69] D. M. Knotter, G. Blasse, J. P. M. van Vliet, G. van Koten, *Inorg. Chem.* **1992**, *31*, 2196.
[70] N. P. Rath, E. M. Holt, K. Tanimura, *Inorg. Chem.* **1985**, *24*, 3934.
[71] F. H. Allen, O. Kennard, *Chem. Des. Autom. News* **1993**, *8*, 31.
[72] A. Bondi, *J. Phys. Chem.* **1964**, *68*, 441.
[73] R. Ahlrichs, J. Besinger, A. Eichhofer, D. Fenske, A. Gbureck, *Angew. Chem.* **2000**, *112*, 4089; *Angew. Chem. Int. Ed.* **2000**, *39*, 3929.
[74] A. Muller, B. Neumuller, K. Dehnicke, *Angew. Chem.* **1997**, *109*, 2447; *Angew. Chem. Int. Ed. Engl.* **1997**, *36*, 2350.
[75] G. Boche, F. Bosold, M. Marsch, K. Harms, *Angew. Chem.* **1998**, *110*, 1779; *Angew. Chem. Int. Ed.* **1998**, *37*, 1684.
[76] I. C. Hayes, A. J. Stone, *Mol. Phys.* **1984**, *53*, 83.
[77] A. J. Stone, *The Theory of Intermolecular Forces*, Clarendon, Oxford, **1996**.
[78] S. Kristyan, P. Pulay, *Chem. Phys. Lett.* **1994**, *229*, 175.
[79] P. Pyykkö, W. Schneider, A. Bauer, A. Bayler, H. Schmidbaur, *Chem. Commun.* **1997**, 1111.
[80] J. M. Poblet, M. Bénard, *Chem. Commun.* **1998**, 1179.
[81] D. Braga, E. D'Oria, F. Grepioni, F. Mota, J. J. Novoa, C. Rovira, *Chem. Eur. J.* **2002**, *8*, 1163.
[82] D. Braga, L. Maini, F. Grepioni, F. Mota, C. Rovira, J. J. Novoa, *Chem. Eur. J.* **2000**, *6*, 4536.
[83] M. A. Carvajal, J. J. Novoa, **2003**, unpublished results.
[84] J. J. Novoa, M. Planas, C. Rovira, *Chem. Phys. Lett.* **1996**, *251*, 33.
[85] J. J. Novoa, M. Planas, M.-H. Whangbo, *Chem. Phys. Lett.* **1994**, *225*, 240.
[86] F. B. van Duijneveldt, J. G. C. M. van Duijneveldt-van de Rijdt, J. H. van Lenthe, *Chem. Rev.* **1994**, *94*, 1873.
[87] D. Braga, F. Grepioni, E. Tagliavini, J. J. Novoa, *New J. Chem.* **1998**, *22*, 755.
[88] L. Pauling, *The Nature of the Chemical Bond*, 3rd ed., Cornell University Press, Ithaca, NY, **1960**.
[89] R. E. Del Sesto, J. S. Miller, P. Lafuente, *Chem. Eur. J.* **2002**, *8*, 4894.
[90] J. J. Novoa, P. Lafuente, R. E. Del Sesto, J. S. Miller, *Angew. Chem.* **2001**, *113*, 2608; *Angew. Chem. Int. Ed.* **2001**, *40*, 2540.
[91] J. J. Novoa, P. Lafuente, R. E. Del Sesto, J. S. Miller, *CrystEngComm* **2002**, *4*, 373.
[92] T. H. Dunning, Jr., *J. Chem. Phys.* **1989**, *90*, 1007.
[93] M. Dolg, U. Wedig, H. Stoll, H. Preuss, *J. Chem. Phys.* **1987**, *86*, 866.
[94] A. Schaefer, H. Horn, R. Ahlrichs, *J. Chem. Phys.* **1992**, *97*, 2571.
[95] S. F. Boys, F. Bernardi, *Mol. Phys.* **1970**, *19*, 553.
[96] B. Neumann, U. Siemeling, H.-G. Stammler, U. Vorfeld, J. G. P. Delis, P. W. N. M. van Leewuen, K. Vrieze, J. Fraaanje, K. Goubitz, P. Zanello, *J. Chem. Soc. Dalton Trans.* **1997**, 4705.
[97] P. C. Healy, J. D. Kildea, B. W. Skelton, A. H. White, *Aust. J. Chem.* **1989**, *42*, 115.
[98] M. K. Ehlert, S. J. Rettig, A. Storr, R. C. Thompson, J. Trotter, *Can. J. Chem.* **1990**, *68*, 1444.
[99] J. S. Thompson, J. F. Whitney, *Acta Crystallogr. Sect. C* **1984**, *40*, 756.
[100] M. K. Ehlert, S. J. Rettig, A. Storr, R. C. Thompson, J. Trotter, *Can. J. Chem.* **1992**, *70*, 2161.
[101] P. C. Healy, J. D. Kildea, A. H. White, *Aust. J. Chem.* **1989**, *42*, 137.
[102] K. Jin, X. Huang, L. Pang, J. Li, A. Appel, S. Wherland, *Chem. Commun.* **2002**, 2872.
[103] G. O. Tan, K. O. Hodgson, B. Hedman, G. R. Clark, M. L. Garrity, T. N. Sorrell, *Acta Crystallogr. Sect. C* **1990**, *46*, 1773.
[104] R. F. Carina, G. Bernardinelli, A. F. Williams, *Angew. Chem.* **1993**, *105*, 1483; *Angew. Chem. Int. Ed. Engl.* **1993**, *32*, 1463.
[105] I. Sanyal, K. D. Karlin, R. V. Strange, N. J. Blackburn, *J. Am. Chem. Soc.* **1993**, *115*, 11259.
[106] T. N. Sorrell, D. L. Jameson, *J. Am. Chem. Soc.* **1983**, *105*, 6013.
[107] R. D. Köhn, G. Seifert, Z. Pan, M. F. Mahon, G. Kociok-Köhn, *Angew. Chem.* **2003**, *115*, 818; *Angew. Chem. Int. Ed.* **2003**, *42*, 793.
[108] D. D. LeCloux, S. J. Lippard, *Inorg. Chem.* **1997**, *36*, 4035.

Received: June 20, 2003
Revised: December 23, 2003 [F5249]